NEOPLASIA
www.neoplasia.com

Volume 17 Number 7 July 2015 pp. 564–573 564

Sorafenib Sensitizes Glioma Cells to the BH3 Mimetic ABT-737 by Targeting MCL1 in a STAT3-Dependent Manner[1,2]

Irina Kiprianova*, Janina Remy*, Nelli Milosch*, Isabelle V. Mohrenz*, Volker Seifert†, Achim Aigner‡ and Donat Kögel*

*Experimental Neurosurgery, Goethe University Hospital, Frankfurt am Main, Germany; †Dept. of Neurosurgery, Goethe University Hospital, Frankfurt am Main, Germany; ‡Rudolf-Boehm-Institute for Pharmacology and Toxicology, Clinical Pharmacology, University of Leipzig, Leipzig, Germany

Abstract

The oncogenic transcription factor signal transducer and activator of transcription 3 (STAT3) is overactivated in malignant glioma and plays a key role in promoting cell survival, thereby increasing the acquired apoptosis resistance of these tumors. Here we investigated the STAT3/myeloid cell leukemia 1 (MCL1) signaling pathway as a target to overcome the resistance of glioma cells to the Bcl-2-inhibiting synthetic BH3 mimetic ABT-737. Stable lentiviral knockdown of MCL1 sensitized LN229 and U87 glioma cells to apoptotic cell death induced by single-agent treatment with ABT-737 which was associated with an early activation of DEVDase activity, cytochrome c release, and nuclear apoptosis. Similar sensitizing effects were observed when ABT-737 treatment was combined with the multikinase inhibitor sorafenib which effectively suppressed levels of phosphorylated STAT3 and MCL1 in MCL1-proficient LN229 and U87 glioma cells. In analogous fashion, these synergistic effects were observed when we combined ABT-737 with the STAT3 inhibitor WP-1066. Lentiviral knockdown of the activating transcription factor 5 combined with subsequent quantitative polymerase chain reaction analysis revealed that sorafenib-dependent suppression of MCL1 occurred at the transcriptional level but did not depend on activating transcription factor 5 which previously had been proposed to be essential for MCL1-dependent glioma cell survival. In contrast, the constitutively active STAT3 mutant STAT3-C was able to significantly enhance MCL1 levels under sorafenib treatment to retain cell survival. Collectively, these data demonstrate that sorafenib targets MCL1 in a STAT3-dependent manner, thereby sensitizing glioma cells to treatment with ABT-737. They also suggest that targeting STAT3 in combination with inducers of the intrinsic pathway of apoptosis may be a promising novel strategy for the treatment of malignant glioma.

Neoplasia (2015) 17, 564–573

Introduction

Gliomas are the most common primary brain tumors in humans. Glioblastoma multiforme is the highest-grade, most aggressive, and frequent glioma [1,2]. A major hallmark of malignant gliomas is their diffuse infiltrative growth into the surrounding brain tissue which renders complete tumor resection impossible [3]. Combined radiotherapy and chemotherapy prolong survival of glioblastoma multiforme patients for several months [4,5], but eradication of residual tumor cells is severely hampered by their intrinsic apoptosis resistance [6], which significantly contributes to the invariable manifestation of tumor recurrence. Therefore, experimental approaches designed to reactivate cell death in apoptosis-refractory malignant glioma have important implications for the development of novel glioma therapies.

Abbreviations: ATF5, activating transcrpition factor 5; MCL1, myeloid cell leukemia 1; STAT3, signal transducer and activator of transcription 3

Address all correspondence to: Donat Kögel, Experimental Neurosurgery, Neuroscience Center, Theodor-Stern-Kai 7, Goethe University Hospital, 60590 Frankfurt am Main.
E-mail: koegel@em.uni-frankfurt.de

[1] The authors declare no conflict of interest.

[2] Financial information: This work was supported by a grant from the Deutsche Forschungsgemeinschaft (DFG, KO 1898 9/1, AI 24/13-1) to D. K. and A. A. and the Deutsche Krebshilfe (grant 108795) to D. K.
Received 17 February 2015; Revised 23 June 2015; Accepted 2 July 2015

1476-5586
http://dx.doi.org/10.1016/j.neo.2015.07.003

The oncogenic transcription factor signal transducer and activator of transcription 3 (STAT3), a component of the Janus-activated kinase (JAK)/STAT3 signaling pathway, is involved in a wide variety of physiological and pathophysiological processes [7,8]. STAT3 is mainly activated via tyrosine phosphorylation (Tyr705) by growth factor/cytokine receptors and non–receptor tyrosine kinases, leading to STAT3 dimerization, nuclear translocation, and subsequent activation of various STAT3 target genes that modulate cell survival, migration, invasion, immune evasion, and angiogenesis [8]. In glioma, activation of STAT3 positively correlates with tumor malignancy [9,10] and predicts a poor clinical outcome [11]. We and others have previously demonstrated the essential function of STAT3 for the highly apoptosis-resistant, proinvasive phenotype of malignant glioma *in vitro* and *in vivo* [12–16].

Pro- and antiapoptotic members of the Bcl-2 family are other key regulators of the mitochondrial (intrinsic) pathway of apoptosis [17]. The Bcl-2 protein family is comprised of three subgroups: 1) the proapoptotic Bax-like proteins (Bax, Bak), 2) the Bcl-2–like proteins [Bcl-2, Bcl-xL, Bcl-W, myeloid cell leukemia 1 (MCL1)], and 3) the proapoptotic BH3-only proteins (Bad, Bim, Bid, etc.), which serve to couple diverse stress stimuli to the intrinsic apoptosis pathway [17,18]. During apoptosis, Bax and Bak trigger mitochondrial outer membrane permeabilization, which is required for the release of proapoptotic factors from the mitochondria into the cytosol. In nonapoptotic cells, Bax and Bak are kept in check by direct binding of the antiapoptotic Bcl-2–like proteins [17–19].

Ever since the molecular cloning of Bcl-2 by Korsmeyer and colleagues, there has been a tremendous interest in the role of Bcl-2 and its homologues in drug resistance and their exploitation as drug targets [20]. Prosurvival Bcl-2 family members are known to be overexpressed in a wide variety of human malignancies, and small molecule inhibitors of Bcl-2–like proteins, also termed BH3 mimetics, are perceived to be highly promising anticancer drugs [21,22]. The most advanced and best characterized synthetic Bcl-2 inhibitor is the Bad-like BH3 mimetic ABT-737 [23] and its orally applicable derivative ABT-263 [24,25], which is currently investigated in a number of clinical phase I/II studies (https://clinicaltrials.gov). Structurally, the prosurvival Bcl-2 family members can be divided into two categories. Bcl-2, Bcl-xL, and Bcl-w are structurally closely related, whereas the accessibility of the BH3 binding pocket of MCL1 (and the less well studied Bcl-2 family member A1) is structurally different from the other three family members. ABT-737 effectively inhibits the antiapoptotic functions of Bcl-2, Bcl-xL, and Bcl-W but fails to target MCL1 [21]. Therefore, MCL1 plays a pivotal role in resistance to Bcl-2/Bcl-xL/Bcl-w-specific inhibitors such as ABT-737.

The multikinase inhibitor sorafenib (Nexavar, Bayer HealthCare Pharmaceuticals, Whippany, NJ, USA) has originally been developed as a RAF inhibitor but also targets several tyrosine kinase receptors. Sorafenib is an orally available drug that is currently under clinical testing in numerous trials including treatment of glioblastoma patients. Here we demonstrate that sorafenib targets MCL1 and efficiently synergizes with ABT-737 to trigger apoptosis in glioma cells. Furthermore, we identify STAT3 as a key upstream regulator of MCL1 and demonstrate the pivotal role of the STAT3/MCL1 signaling axis in apoptosis resistance of glioma.

Materials and Methods

Reagents

ABT-737, sorafenib, and WP-1066 (pStat3 inhibitor III) were obtained from Santa Cruz, Heidelberg, Germany. z-Val-Ala-DL-Asp-fluoromethylketone was from Bachem (Weil am Rhein, Germany). Cell culture medium (Dulbecco's modified Eagle's medium) and supplements were purchased from Invitrogen (Darmstadt, Germany). All other biochemicals and chemicals were provided in analytical-grade purity from Roth (Karlsruhe, Germany) or Sigma-Aldrich (Seelze, Germany).

Cell Culture and Lentiviral Transduction

All experiments were performed in the human glioma cell lines LN229, U343, and U87 [25,26]. MCL1 (SHCLNV-NM_021960) and activating transcription factor 5 (ATF5) (SHCLNV-NM_012068) [27] were silenced by transduction-ready shRNA lentiviral particles (Sigma-Aldrich) according to the manufacturer's instructions. The target sets included five sequences encoding different small hairpins. The pLKO.1-puro control transduction particles (SHC001V) did not contain a hairpin insert and were used as a negative control. Transduction and selection of stable cells were performed as described previously [26].

Transfection

U87 and LN229 cells were seeded into six-well plates and allowed to grow overnight until 70% to 80% confluence. Then, cultures were transfected with myr-AKT1 [*Akt1* cDNA (activated) in pUSeamp; Millipore, Darmstadt, Germany] or with pYN3218-Stat3C [28] using transfection reagent Metafectene (Biontex, München, Germany) according to the manufacturer's instructions. Cells were harvested 48 hours posttransfection for further Western blot analysis.

Immunoblotting

For Western blots, cells cultivated in 75-cm^2 cell culture flasks were lysed with SDS lysis buffer including protease and phosphatase inhibitors. Protein content was quantified with the BC Assay Kit from Uptima (Mannheim, Germany). Eighty micrograms of protein was loaded onto a 12% polyacrylamide gel followed by gel electrophoresis. Proteins were transferred onto nitrocellulose membranes that were incubated with an anti-MCL1, anti-BAK antibody (S-19, Santa Cruz, Heidelberg, Germany), anti-pSTAT3 (Tyr705) antibody, anti-AKT antibody, anti-STAT3 antibody, anti-BAX, anti-BCL2, anti-BCL-XL (all from Cell Signaling, Bad Homburg, Germany), or an anti-GAPDH antibody (Calbiochem, Darmstadt, Germany). After washing, blots were incubated with a secondary IRDye 800CW goat anti-mouse antibody followed by detection with an Odyssey Infrared Imaging System (LI-COR, Bad Homburg, Germany).

RNA Isolation and Quantitative Polymerase Chain Reaction (qPCR)

Cells were cultivated in 75-cm^2 cell culture flasks until subconfluency. RNA isolation was performed by using the RNAeasy Plus Mini Kit according to the manufacturer's instructions (Qiagen, Hilden, Germany). In the procedure, a DNAse digestion step was included. RNA content was photometrically measured with a BioPhotometer (Eppendorf, Hamburg, Germany). One microgram of RNA was used for cDNA synthesis in a 20-µl volume with SuperScript III Reverse Transcriptase (Invitrogen, Darmstadt, Germany). Quantitative PCR was performed with the TaqMan Gene Expression Assay using 25 ng of cDNA per reaction. Analysis was carried out in an ABI PRISM 5700 Sequence Detection System (Applied Biosystems, Darmstadt, Germany) with the OneStep Plus Software. Analysis of relative gene expression data was performed by employing the $2^{-\Delta\Delta C(t)}$ method.

Caspase 3-Like Enzymatic Activity Assay

For measuring effector caspase activity, treated cells were lysed in 200 µl of lysis buffer [10 mmol/l HEPES (pH 7.4), 42 mmol/l KCl,

5 mmol/l MgCl2, 1 mmol/l phenylmethylsulfonyl fluoride, 0.1 mmol/l EDTA, 0.1 mmol/l EGTA, 1 mmol/l DTT, 1 μg/mL pepstatin A, 1 μg/mL leupeptin, 5 μg/mL aprotinin, 0.5% 3-(3-cholamidopropyldimethylammonio)-1-propane sulfonate (CHAPS)]. Fifty microliters of this lysate was added to 150 μl of reaction buffer [25 mmol/l HEPES, 1 mmol/l EDTA, 0.1% CHAPS, 10% sucrose, 3 mmol/l DTT (pH 7.5)]. The fluorigenic substrate Ac-DEVD-AMC was added at a final concentration of 10 μmol/l. Accumulation of AMC fluorescence was monitored over 2 hours using a TECAN fluorescent plate reader (Tecan, Crailsheim, Germany; excitation 380 nm, emission 465 nm). Protein content was determined using the Pierce Coomassie Plus Protein Assay reagent (Fisher Scientific, Schwerte, Germany). Caspase activity was expressed as a change in fluorescence units per microgram of protein per hour.

MTT Cell Viability Assay

MTT (3-(4,5-dimethylthiazol-2-yl)-2,5-diphenyltetrazolium bromide, Sigma Aldrich) working solution (5 mg/ml) was prepared by dissolving MTT in PBS following sterile filtration. One day before treatment, 2000 cells/well were plated in a transparent flat-bottom 96-well tissue culture plate in a total volume of 100 μl/well. At least eight technical replicates were used for each condition. After the appropriate incubation time, 20 μl of MTT solution was added (final concentration: 0.83 mg/ml) and incubated for 3 hours at 37°C, 5% CO_2. After carefully removing the medium, 100 μl of 2-propanol was added to dissolve the formazan salt. Absorbance was measured at 560 nm with a GENios fluorescence plate reader (Tecan, Mainz, Germany).

Flow Cytometry

For flow cytometric detection, 20,000 cells/well were seeded in 24-well microtiter plates and subjected to the appropriate treatment. Next, they were washed and trypsinized. Detached cells and trypsinized adherent cells were collected, pooled, and centrifuged. The cell pellet was resuspended in 50 μl HEPES buffer (10 mM Hepes/NaOH, pH 7.4, 140 mM NaCl, 5 mM $CaCl_2$) and stained with propidium iodide (Sigma-Aldrich) and Annexin V (Roche, Mannheim, Germany). After a 10-minute incubation, samples were analyzed in a BD FACS Canto II (BD Biosciences, Heidelberg, Germany) using FACS Diva Software.

Immunofluorescence Staining for Confocal Microscopy

A total of 20,000 cells/well were plated in a 24-well plate on cover slips (13 mm) and were allowed to adhere for 24 hours. All treatments were performed in a final volume of 500 μl. Following treatment, cells were first washed twice with ice-cold PBS, fixed in 500 μl paraformaldehyde (4% PFA) for 10 minutes, and permeabilized for 3 minutes with ice-cold 0.1% Triton X-100 in PBS. After subsequent washing steps, unspecific binding was blocked by 5% horse serum and 0.3% Triton X-100. Anti–cytochrome c, (BD Pharmingen) was applied in 1% horse serum and 0.3% Triton X-100 in PBS. Afterwards, cells were washed twice with ice-cold PBS. For secondary antibody incubation. Cy3-conjugated Donkey Anti-Mouse IgG (Dianova, Hamburg, Germany) was diluted in 1% horse serum and 0.3% Triton X-100 in PBS, and samples were incubated while gently shaking at room temperature in the dark and washed with ice-cold PBS. Cellular nuclei were stained with the monomeric cyanine nucleic acid stain TO-PRO-3 (Life Technolgies, Darmstadt, Germany) at a final concentration of 1 μmol/l in PBS for 10 minutes. Images were acquired with a Nikon Eclipse TE2000-S fluorescence microscope coupled to a DS-5Mc cooled color digital camera (Nikon, Düsseldorf, Germany) and NIS Elements AR (version 3.22) software from Nikon (TO-PRO-3: excitation 642 nm, emission 662 nm; Cy3: excitation 554 nm, emission 568 nm).

Immunoprecipitation

For examination of the activation status of Bax, we employed immunoprecipitation with μMACS Protein A/G MicroBeads (Miltenyi Biotec, Bergisch Gladbach, Germany). Briefly, after harvesting and washing, cells were pelleted and lysed with CHAPS buffer [1% CHAPS (Sigma), 10 mM HEPES, pH 7.4, 150 mM NaCl], supplemented with Protease Inhibitor Cocktail (Roche) on ice for 25 minutes followed by centrifugation at 14,000 rpm for 25 minutes at 4°C. A mouse monoclonal antibody against active BAX (6A7, Enzo Life Sciences, Lörrach, Germany) and 50 μl of Protein A/G MicroBeads were added to 500 μg of protein in 400 μl CHAPS buffer, and samples were incubated under rotation at 4°C overnight. Elution of immune complexes was performed according to the manufacturers' protocol (Miltenyi Biotec). Finally, the eluted precipitates were analyzed by SDS-PAGE with an anti-BAX antibody and anti-GAPDH antibody.

Statistics

Results are expressed as mean ± SEM. All experiments were repeated at least three times, yielding similar results. Statistical analyses were performed using SPSS (IBM, Armonk, NY) with one-way analysis of variance followed by Tukey's honestly significant difference *post hoc* comparisons. P values $<.05$ were considered as statistically significant.

Results

Knockdown of MCL1 and ABT-737–Induced Apoptosis

To analyze the putative role of MCL1 for cell death resistance of glioma cells, we established a stable lentiviral knockdown of MCL1 in the two glioblastoma cells lines LN229 and U87 (Figure 1*A*). The effect of ABT-737 single-agent treatment (5 μM) was subsequently assayed by flow cytometric quantification of total cell death in a time course experiment (4, 8, 16, and 24 hours). Knockdown of MCL1 evoked a significant increase in ABT-737–induced cell death in LN229 cells (Figure 1*B*). We also observed a moderate induction of cell death in MCL1-proficient LN229 wt cells. In LN229 MCL1 KD cells, ABT-737 induced a transient activation of effector caspases, peaking at 4 to 8 hours (Figure 1*C*, *left panel*). In line with this observation, an MTT viability assay revealed a significantly lower MTT activity after treatment with ABT-737 in LN229 MCL1-KD cells which could be rescued with the pan-caspase-inhibitor zVAD (Figure 1*C*, *right panel*). The potentiating effect of the MCL1 knockdown on ABT-737–induced apoptosis was also confirmed in U87 cells (Figure 1*D*). To rule out possible off-target effects of the applied shRNA, we also transiently knocked down MCL1 with two different siRNA oligos. In analogy to the data obtained with the stable knockdowns of MCL1, both siRNas significantly enhanced effector caspase activity and cell death in response to ABT-737 (Suppl. Figure 1, *A*–*C*). Collectively, these data provide evidence that, in glioma cells, MCL1 confers resistance to apoptotic cell death induced by ABT-737.

Synergistic Induction of Apoptosis by Sorafenib and ABT-737

To pharmacologically target MCL1 in wild-type cells, we employed the multikinase inhibitor sorafenib (final concentration 5 μM), which almost completely depleted protein levels of MCL1 as

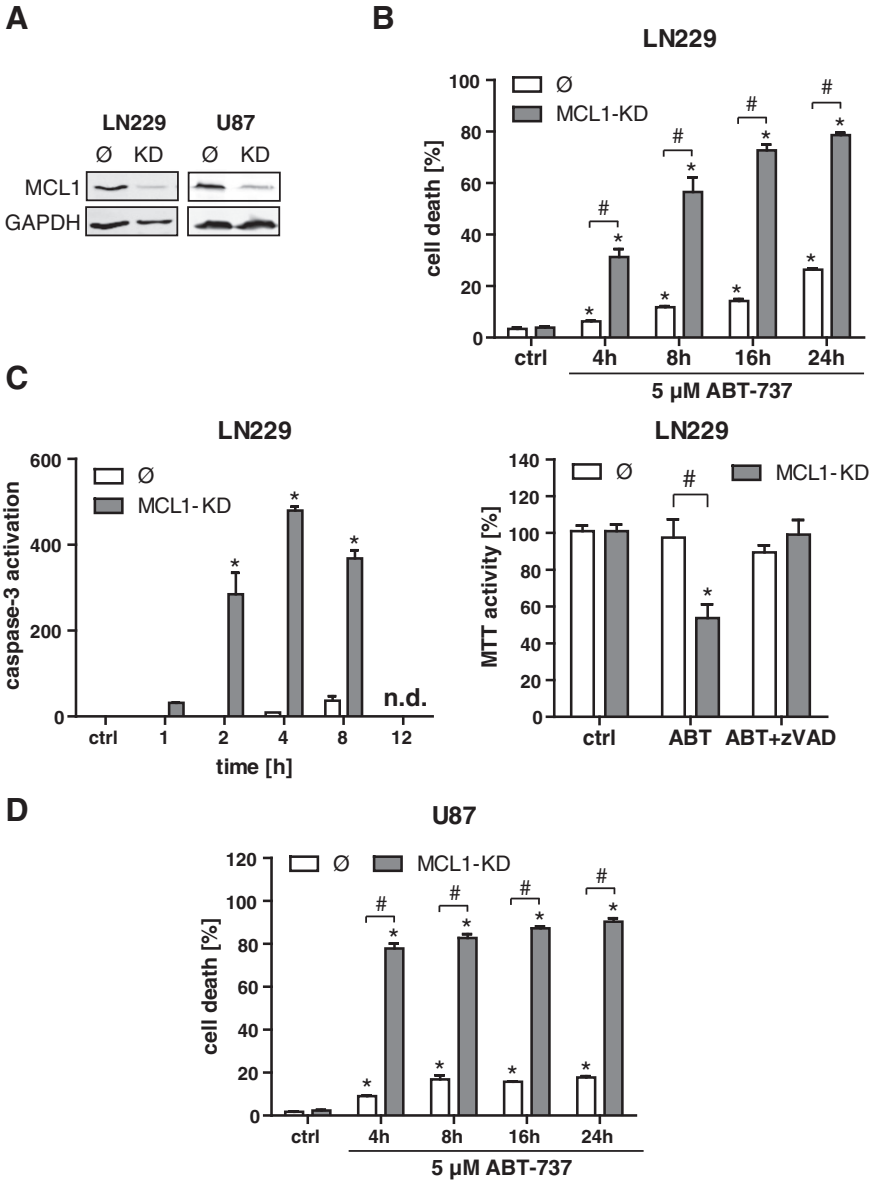

Figure 1. MCL1 knockdown sensitizes glioma cell lines to ABT-737–induced apoptotic cell death. Establishment of a stable lentiviral MCL1 knockdown in LN229 and U87 glioma cell lines, as determined by Western blotting (A). LN229 control cells (Ø) and MCL1-KD cells were treated with 5 μM ABT-737 in a time course experiment (4, 8, 16, and 24 hours), and cell death was quantified by FACS analysis of Annexin/PI (B). Effector caspase activation as determined by DEVD cleavage in LN229 empty vector control cells (Ø) and MCL1-KD cells after treatment for 1, 2, 4, 8, and 12 hours with 5 μM ABT-737 (C, left panel). Analysis of MTT activity in LN229 empty vector control cells (Ø) and MCL1-KD cells after treatment with 5 μM ABT-737 for 24 hours (C, right panel). Where indicated, cells were additionally treated with the pan-caspase inhibitor zVAD. U87 control cells (Ø) and MCL1-KD cells were treated with 5 μM ABT-737 in a time course experiment (4, 8, 16, and 24 hours), and cell death was quantified by FACS analysis of Annexin/PI (D). In all parts of the figure, graphs represent means of n = 4-8 cultures + SEM. *P < .05, significant difference to untreated controls; #P < .05, significant difference to respective control cell line.

early as 4 hours after treatment (Figure 2*A*). Sorafenib did not detectably affect the expression of the other Bcl-2 family members BCL-xL, BAK, and BAX but significantly suppressed the expression of Bcl-2. FACS analysis of Annexin binding/PI uptake confirmed that LN229 MCL1-KD cells were more sensitive to ABT-737–induced cell death (Figure 2*B*), with a prominent shift to Annexin-positive and Annexin/PI-positive cells that was not seen in the LN229 control cell line (Figure 2*B*). Another time course analysis performed after 4, 8, 16, and 24 hours revealed that, whereas sorafenib alone exerted no effect, the double treatment with ABT-737 and sorafenib efficiently triggered apoptosis in LN229 control cells (Figure 2, *B* and *C*, *left panel*) to a level well above ABT-737 alone (compare Figure 1*B*). This was associated with enhanced caspase induction (Figure 2*C*, *right panel*). Similar sensitizing effects of sorafenib were also observed in MCL1-proficient U87 control cells (Figure 2*D*). The MCL1-KD evoked an earlier shift to cell death after combined treatment with ABT-737 and sorafenib in both cell lines (Figure 2, *C*, *left panel*, and *D*). Single-agent treatment with sorafenib was not sufficient to induce cell death in LN229 cells under these experimental conditions, whereas it triggered moderate cell death in U87 control cells and U87

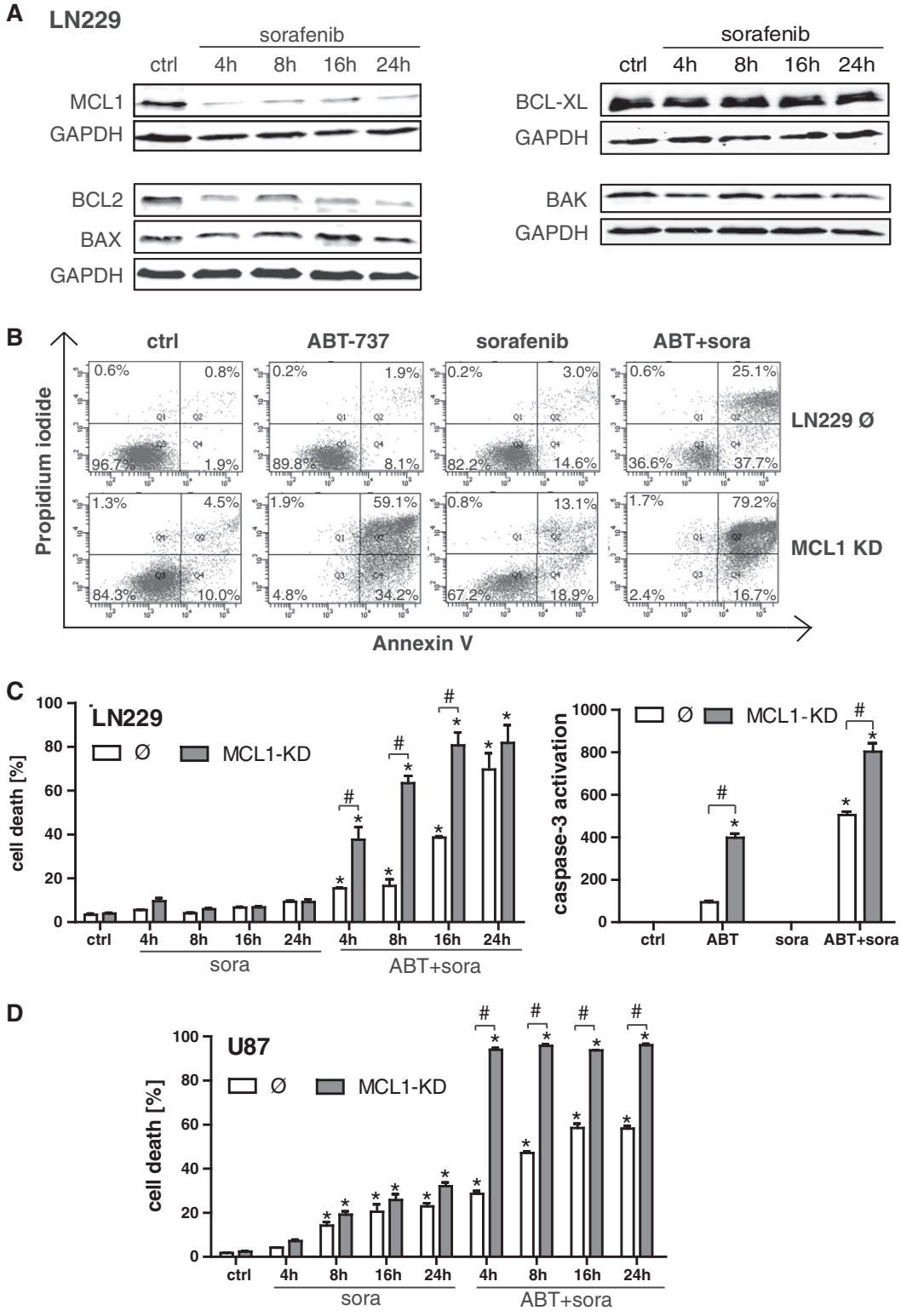

Figure 2. Sorafenib targets MCL1 and synergizes with ABT-737 to induce apoptosis in glioma cells. LN229 cells were treated with 5 μM sorafenib for the time periods indicated, and MCL1, BCL-2, BCL-XL, BAX, and BAK expression levels were subsequently analyzed by Western blotting. Western blots were repeated two times with similar results (A). Representative histograms of LN229 control cells (Ø) and LN229 MCL1-KD cells after treatment for 24 hours with 5 μM ABT-737, 5 μM sorafenib, or combined treatment as analyzed by Annexin V/PI staining and flow cytometry analysis (B). For a time course analysis, cultures of LN229 control cells (Ø) and LN229 MCL1-KD cells were treated with 5 μM sorafenib +/− 5 μM ABT-737 for 4, 8, 16, and 24 hours (C, left panel). Effector caspase activation was analyzed after single treatment with 5 μM ABT-737 or 5 μM sorafenib, or combined treatment for 4 hours (C, right panel). Cultures of U87 control cells (Ø) and LN229 MCL1-KD cells were treated with 5 μM sorafenib +/− 5 μM ABT-737 for 4, 8, 16, and 24 hours and analyzed by Annexin V/PI staining and flow cytometry analysis (D). All graphs represent means of $n = 4$ cultures + SEM; $*P < .05$, significant difference to untreated controls; $\#P < .05$, significant difference to respective control cell line. Experiments were repeated at least 2 times with similar results.

MCL1-KD cells (Figure 2, *C*, *left panel*, and D). However, under MCL1-KD conditions, sorafenib contributed in both cell lines only to a minor extent to the profound ABT-737 effects (compare Figures 2*C* vs. 1*B*, 2*D* vs. 1*D*), thus confirming that sorafenib acts to a large extent via suppression of MCL1 in glioma cells.

To confirm activation of apoptotic cell death, we also analyzed nuclear condensation/fragmentation and mitochondrial cytochrome c release of LN229 control cells and LN229 MCL1-KD cells after treatment with sorafenib, ABT-737, and combined treatment with both drugs on the single-cell level (Figure 3, *A* and *B*). In line with the FACS analyses (Figure 2, *B* and *C*), nuclear apoptosis and cytochrome c release to the cytosol were observed after ABT-737 single-agent treatment in LN229 MCL1-KD cells and after combined treatment in LN229 control cells, which were further enhanced in MCL1-KD cells (Figure 3, *A* and *B*).

MCL1 Overexpression Is Independent of ATF5

It was previously proposed that the CREB3L2/RAF/ATF5/MCL1 pathway plays a pivotal role in driving the overexpression of MCL1 in glioma [27]. To further scrutinize the importance of this pathway for MCL1-driven cell death resistance, we established a stable lentiviral knockdown of ATF5 in both cell lines (LN229, U87; Figure 4*A*, *left panel*). Unexpectedly, the knockdown of ATF5 had no discernible effect on basal protein expression levels of MCL1 (Figure 4*A*, *right panel*) as determined by Western blot analysis. qPCR analysis confirmed that knockdown of ATF5 had no major effects on MCL1 mRNA expression (Figure 4, *B* and *C*, *left panels*), indicating that, in the two investigated cell models, ATF5 is not a major driver of MCL1 expression and is therefore not involved in the suppressing effects of sorafenib on MCL1. Of note, sorafenib treatment decreased the MCL1 mRNA levels in LN229 and U87 cells, indicating that, in addition to modulating MCL1 protein stability, it also exerts its suppressing function via inhibition of MCL1 transcription in an ATF5-independent manner. In analogy to the lack of MCL1 regulation, the ATF5 knockdown also did not alter the extent of caspase induction after combined treatment with sorafenib and ABT-737 in both cell lines (Figure 4, *B* and *C*, *right panels*).

Sorafenib Targets MCL1 in a STAT3-Dependent Manner

Given the key function of STAT3 in driving gliomagenesis and glioma cell death resistance, we next analyzed the possible involvement of STAT3 in the MCL1-inhibiting effects of sorafenib. As depicted in Figure 5*A*, LN229 and U87 glioma cells were treated with sorafenib or the STAT3 inhibitor WP-1066 [29] for different time periods. Both drugs were able to reduce levels of MCL1 and phospho-Stat3 in a time-dependent manner. Next, we investigated whether a double treatment with WP-1066 and ABT-737 could mimic the synergizing effects of sorafenib and ABT-737 in LN229 cells (Figure 5*B*). To this end, LN229 control and MCL1-KD cells were treated with WP-1066 and ABT-737 for 4, 16, and 24 hours, and total cell death was subsequently analyzed via flow cytometry after staining with Annexin V and PI. In analogy to sorafenib, WP-1066 was able to exert potent synergistic effects with ABT-737 in LN229 control cells, whereas the MCL1-KD cells revealed a slightly earlier shift to cell death after the combined treatment (Figure 5*B*).

To further analyze the mechanisms underlying sorafenib-mediated MCL1 suppression, a set of transient transfection experiments was performed to evaluate a possible rescue of MCL1 protein expression under sorafenib treatment. First, we examined the involvement of the prosurvival kinase AKT, which is known as a downstream target of sorafenib and an upstream activator of MCL1 [30–32]. For this purpose, we transfected U87 and LN229 cells with a myristoylated, constitutively active mutant of *AKT1* followed by treatment with sorafenib. Transient expression of AKT in glioma cells was confirmed by Western blot analysis showing increased AKT protein levels and moderately elevated levels of MCL1 in *AKT1*-transfected cells compared to mock-transfected controls. However, this pronounced expression of AKT failed to abrogate the suppressing effect of sorafenib on MCL1 protein expression when comparing the 4- and 8-hour time points after treatment (Figure 5*C*).

In light of the synergizing effects of WP-1066 and ABT-737 on cell death, we also examined the potential effects of a constitutively active mutant of STAT3 on MCL1 levels. Cells were transfected with the mutant STAT3-C that does not require tyrosine phosphorylation for its activation [28], and transient expression of STAT3-C was confirmed by Western blot. Interestingly, STAT3-C was able to markedly enhance basal expression levels of MCL1 and to significantly counteract the suppressing effects of sorafenib on MCL1 4 and 8 hours after drug application (Figure 5*D*). Expression of STAT3-C also significantly reduced cell death induced by ABT-737 in combination with sorafenib (Suppl. Figure 1, *D* and *E*). These results suggest that the STAT3/MCL1 axis is an important target involved in the apoptosis-sensitizing effects of the multikinase inhibitor sorafenib in glioma.

Discussion

Increasing evidence supports the central function of STAT3 for gliomagenesis, tumor progression, and therapy resistance of malignant gliomas. STAT3 is known to exert pleiotropic effects on different tumor cell autonomous functions and the interaction of tumor cells with the tumor microenvironment. One key oncogenic property of STAT3 is its antiapoptotic function that is functionally correlated to the acquired apoptosis resistance of tumor cells. In line with this notion, inhibition of the Stat3 pathway or constitutively active Stat3 was shown to induce apoptosis in glioma cells [16,29].

This study was undertaken to investigate the STAT3/MCL1 signaling axis as a target to overcome the resistance of glioma cells to the BH3 mimetic ABT-737. We have previously demonstrated that the expression of prosurvival Bcl-2 proteins is correlated with cell death resistance of glioma cells and that they represent an attractive target for glioma therapy [26]. The proapoptotic activity of ABT-737 was shown to negatively correlate with MCL1 expression in various cancer models, and suppression of MCL1 expression was demonstrated to abrogate ABT-737 resistance in many types of cancer, for example, in acute myeloid leukemia cells with high endogenous expression of MCL1 [33]. Therefore, the combination of the orally applicable ABT-737 derivative ABT-263 with drugs targeting the expression/stability of MCL1 may be a feasible and elegant approach for cancer therapies.

To further explore the critical function of MCL1 for apoptosis resistance of glioma, we performed a stable lentiviral knockdown of MCL1 that sensitized LN229 and U87 glioma cells to cell death induced by single treatment with ABT-737. This cell death was associated with activation of effector caspases, cytochrome c release from the mitochondria, and nuclear hallmarks of apoptosis.

Concomitantly, combined treatment with ABT-737 and sorafenib, which we demonstrate to efficiently and quickly reduce MCL1 (and to a lesser degree Bcl-2) protein levels, was able to exert synergistic effects on cell death in MCL1-expressing LN229 and U87 cells.

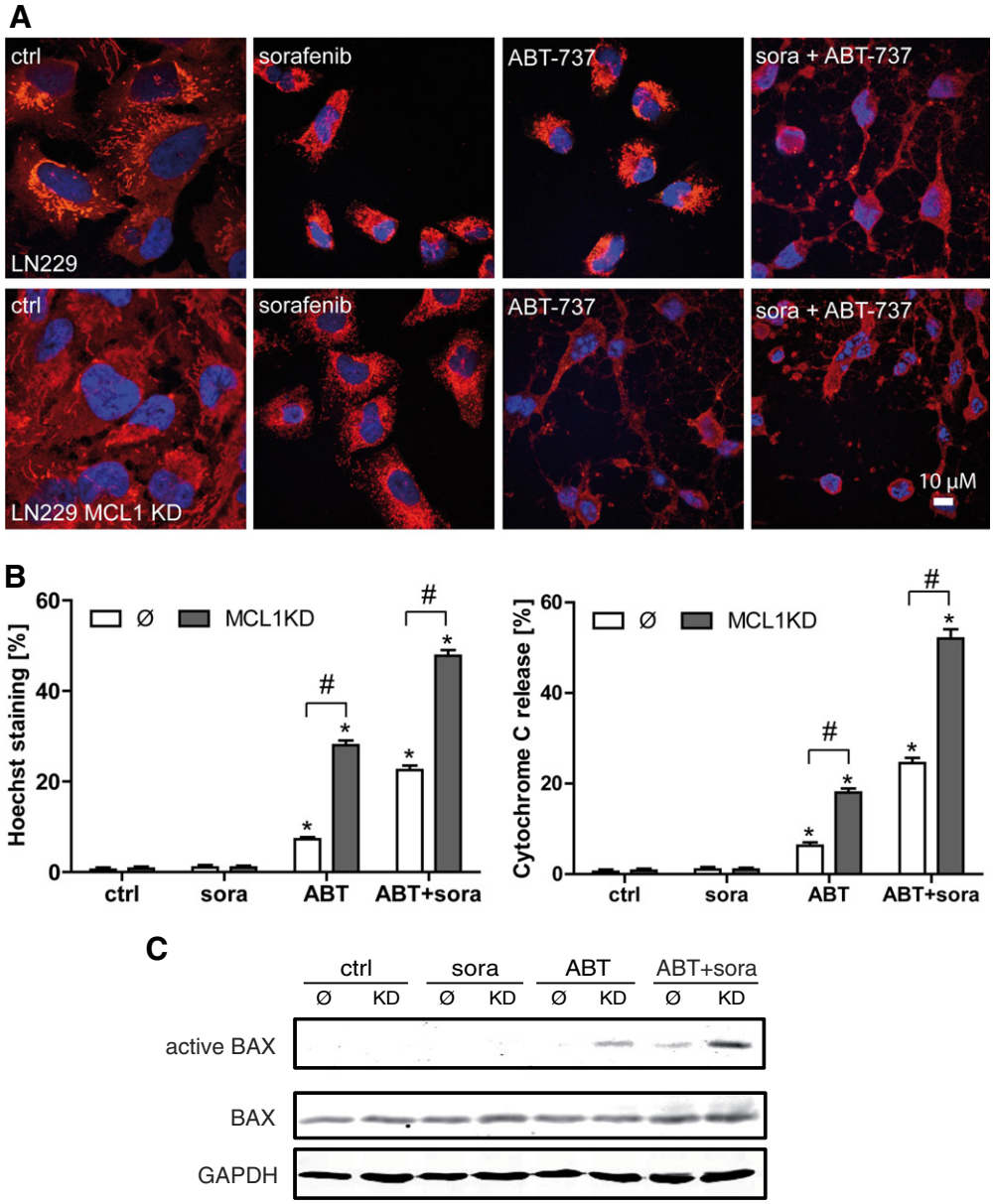

Figure 3. Detection of apoptosis at the single cell level after treatment with ABT-737 and sorafenib. For analysis on the single cell level, LN229 control cells (Ø) and LN229 MCL1 knockdown cells were treated with 5 μM ABT-737 or 5 μM sorafenib, or both agents simultaneously, for 4 hours. After fixation, cells were stained with an anti–cytochrome C antibody. Nuclei were stained with To-Pro (A). Representative images of apoptotic cells are shown. Scale bar: 10 μm. Experiments were repeated three times with similar results. Quantitative assessment of cytochrome C release and nuclear condensation/fragmentation (Hoechst staining) by fluorescence microscopy (B). Data represent means + SEM of 4 independent cultures. One hundred cells were counted for each culture. *$P < .05$, significant difference to untreated controls. #$P < .05$, significant difference to control cell line. Immunoprecipitation of activated BAX in LN229 control cells and MCL1 KD cells (C). Cells were treated as described above.

Because ABT-737 inhibits Bcl-2 and Bcl-xL but fails to target MCL1, suppression of MCL1 is likely the key mechanism of synergism between sorafenib and ABT-737. Importantly, the multikinase inhibitor sorafenib, either alone or in combination with other drugs, is in clinical development for a wide variety of human cancers including glioma (https://clinicaltrials.gov). Synergistic effects of sorafenib with Bcl-2 inhibition were recently also demonstrated for the orally applicable ABT-737 derivative ABT-263 in cancer cells [30]. In this context, several groups also proposed that downregulation of MCL1 sensitizes different cancer cell lines to ABT-737 *in vitro* [34,35]. This is demonstrated in this study.

We next asked the question which upstream signaling components are essential to drive MCL1 overexpression in glioma. In a previous report, a CREB3L2/RAF/ATF5 pathway was proposed to be essential for MCL1 activation and glioma cell survival [27]. Interestingly, although we demonstrate that sorafenib-dependent suppression of MCL1 to a large degree occurs at the transcriptional level, our experiments on the lentiviral knockdown of the transcription factor ATF5 revealed that MCL1 expression does indeed not depend on ATF5.

Instead, we found in our experiments an efficient sorafenib-mediated suppression of MCL1 expression in MCL1-proficient LN229

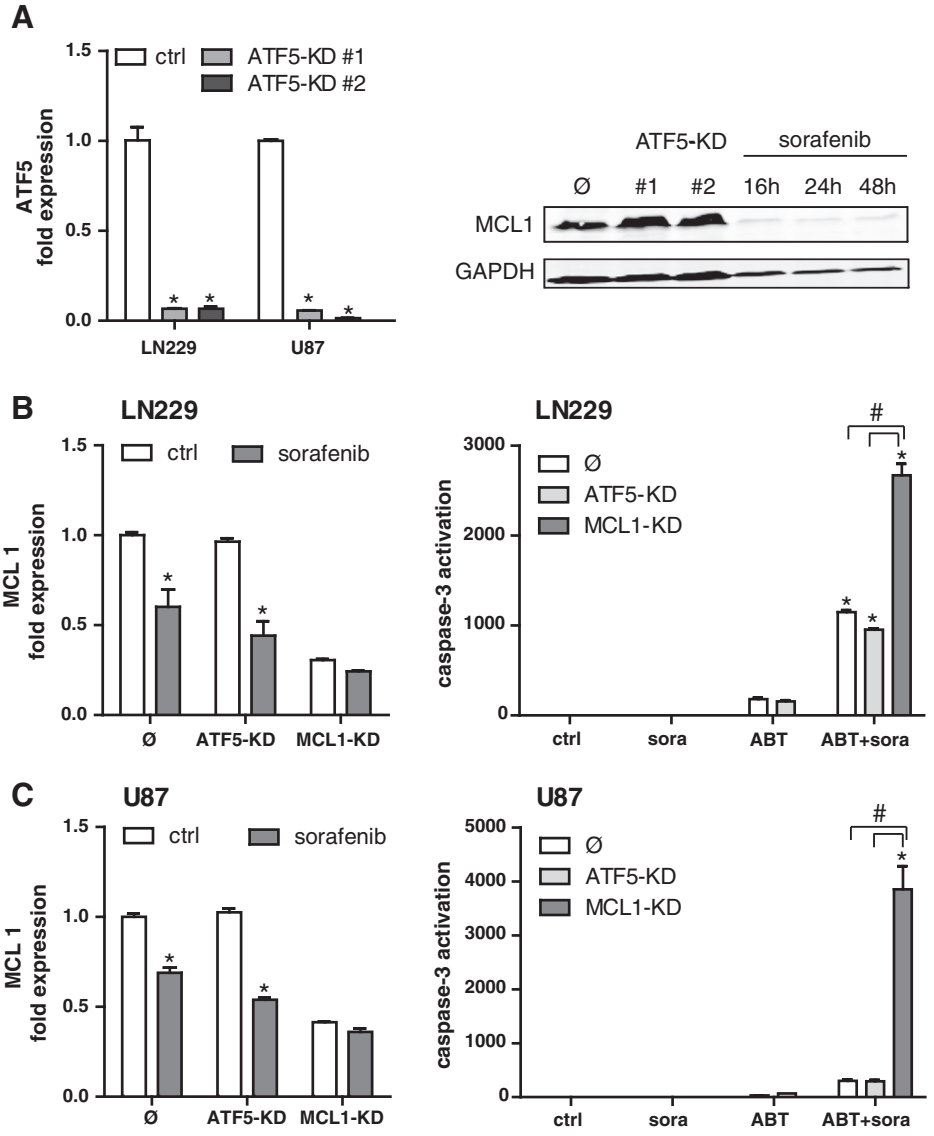

Figure 4. Knockdown of ATF5 has no effect on MCL1 expression and apoptosis sensitivity. Verification of the ATF5 knockdown in LN229 and U87 cells as analyzed by qPCR (A). Two single-cell clones per cell line are shown. Data represent means of $n = 3$ cultures + SEM; $^*P < .05$, significant difference to respective control cell line. MCL1 expression of ATF5 knockdown cells in comparison to LN229 control cells (Ø) as analyzed by Western blotting. GAPDH served as loading control. mRNA levels of MCL1 were assayed by qPCR in control cells with the corresponding knockdown clones of ATF5 and MCL1 in LN229 (B, left panel) and in U87 (C, left panel) +/− treatment with 5 μM sorafenib for 24 hours. Data represent means of $n = 3$ cultures + SEM; $^*P < .05$, significant difference to respective control cell line. Experiments were repeated three times with similar results. Effector caspase activity after treatment for 4 hours with 5 μM sorafenib, 5 μM ABT-737, or the combination of both (C, D, right panels). Experiments were repeated three times with similar results. All graphs represent means of $n = 4$ cultures + SEM; $^*P < .05$, significant difference to untreated controls; $\#P < .05$, significant difference to respective control cell line. n.s.: not significant.

and U87 glioma cells that was tightly associated with reduced activation of STAT3. In line with this, the synergistic effects of sorafenib and ABT-737 described above could be mimicked in our experiments by combination of ABT-737 with the STAT3 inhibitor WP-1066 [29]. Moreover, the constitutively active STAT3 mutant STAT3-C was able to significantly enhance MCL1 levels, thus counteracting the effects of sorafenib and retaining cell survival. In contrast, a constitutively active mutant of AKT failed to sustain MCL1 expression under sorafenib treatment. These findings are in line with a study demonstrating sorafenib-dependent downregulation of pStat3 (Tyr705) and MCL1 expression, whereas the expression of other apoptosis-related proteins (Bcl-2, Bcl-xL, XIAP, survivin) was largely unaltered [36]. Another study confirmed the proapoptotic and STAT3-inhibiting effects of sorafenib and revealed that inactivation of STAT3 by sorafenib occurs via upstream inhibition of the JAK kinases JAK1 and JAK2 and increased phosphatase activity in glioma cells [32], likely involving the participation of the tyrosine phosphatase SHP2 [37].

Conclusions

Collectively, our data demonstrate that sorafenib targets MCL1 in a STAT3-dependent manner, thereby sensitizing glioma cells to treatment with ABT-737. Our results also suggest that targeting STAT3 in combination with inducers of the intrinsic pathway of

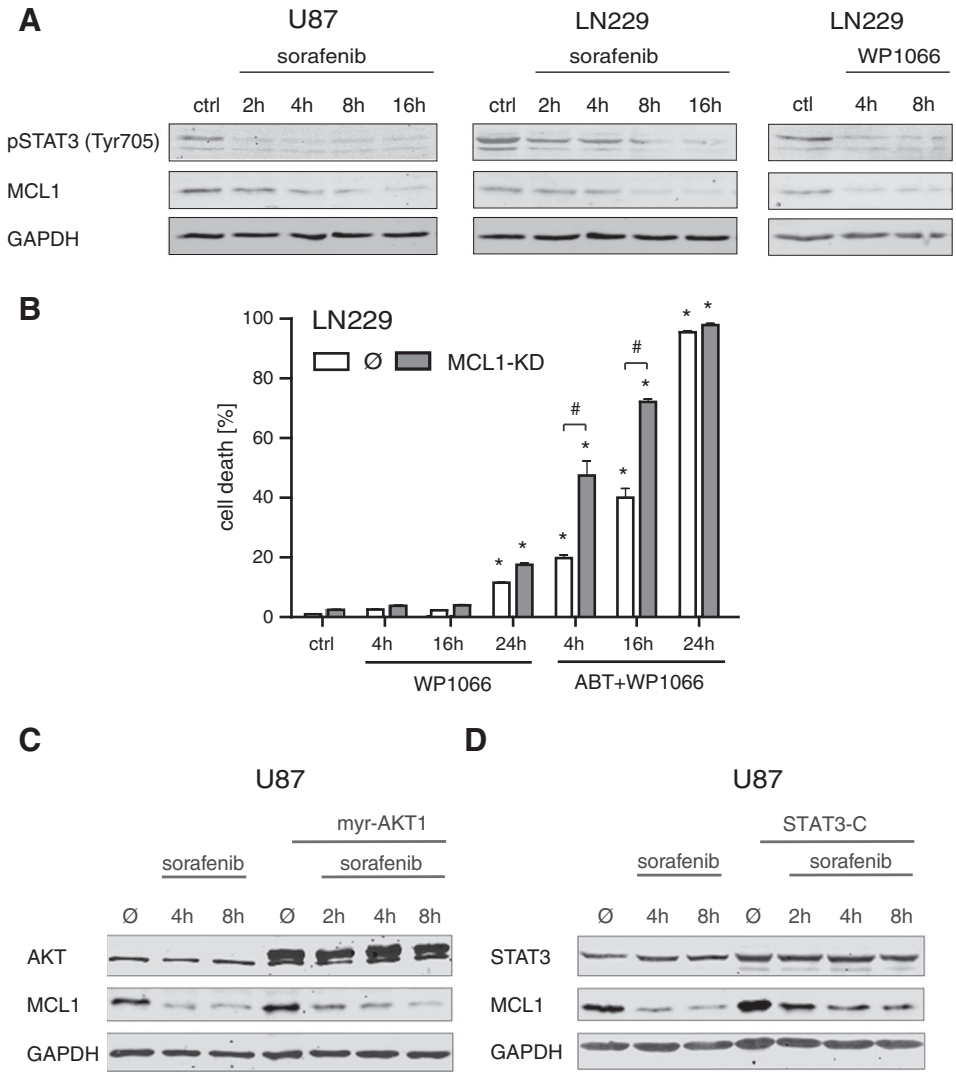

Figure 5. Treatment with the STAT3 inhibitor WP-1066 reduces MCL1 levels and sensitizes MCL1-KD glioma cells to apoptotic cell death after combined treatment with ABT-737. LN229 and U87 glioma cells were treated with 10 μM sorafenib or 10 μM WP-1066 for the indicated time periods and subjected to Western blotting (A). Both drugs reduced MCL1 and phospho-Stat3 expression in a dose-dependent manner. GAPDH was used as loading control. Quantification of cell death (B). LN229 control or MCL1-KD cells were treated with 3 μM WP-1066 +/− 5 μM ABT-737 for the indicated time periods. Total cell death was analyzed via Annexin/PI staining and flow cytometry. Data are means from $n = 4$ cultures + SEM. Statistical significance: *$P < .05$ compared to untreated controls; #$P < .05$ compared to the respective control cell line. Experiments were repeated three times with similar results. Effect of transient overexpression of constitutively active AKT1 (C) and STAT3 (D) on MCL1 protein levels under treatment with 10 μM sorafenib for the indicated time periods. Western blot analysis was performed with transfected U87 cells harvested 48 hours posttransfection. GAPDH was used as loading control. Overexpression of myristoylated AKT1 does not counteract the sorafenib-induced MCL1 downregulation (C). Increased MCL1 protein expression in cells transfected with STAT3-C in comparison to mock-transfected controls, counteracting sorafenib-mediated MCL1 inhibition (D).

apoptosis may be a promising novel strategy for the treatment of malignant glioma.

Supplementary data to this article can be found online at http://dx.doi.org/10.1016/j.neo.2015.07.003.

Acknowledgement

We thank Gabriele Köpf for excellent technical assistance.

References

[1] Louis DN, Ohgaki H, Wiestler OD, Cavenee WK, Burger PC, Jouvet A, Scheithauer BW, and Kleihues P (2007). The 2007 WHO classification of tumours of the central nervous system. *Acta Neuropathol* **114**, 97–109.

[2] Louis DN, Perry A, Burger P, Ellison DW, Reifenberger G, von Deimling A, Aldape K, Brat D, Collins VP, and Eberhart C, et al (2014). International Society of Neuropathology–Haarlem consensus guidelines for nervous system tumor classification and grading. *Brain Pathol* **24**, 429–435.

[3] Claes A, Idema AJ, and Wesseling P (2007). Diffuse glioma growth: a guerilla war. *Acta Neuropathol* **114**, 443–458.

[4] Stupp R, Hegi ME, Mason WP, van den Bent MJ, Taphoorn MJ, Janzer RC, Ludwin SK, Allgeier A, Fisher B, and Belanger K, et al (2009). Effects of radiotherapy with concomitant and adjuvant temozolomide versus radiotherapy alone on survival in glioblastoma in a randomised phase III study: 5-year analysis of the EORTC-NCIC trial. *Lancet Oncol* **10**, 459–466.

[5] Stupp R, Mason WP, van den Bent MJ, Weller M, Fisher B, Taphoorn MJ, Belanger K, Brandes AA, Marosi C, and Bogdahn U, et al (2005). Radiotherapy plus concomitant and adjuvant temozolomide for glioblastoma. *N Engl J Med* **352**, 987–996.

[6] Ziegler DS, Kung AL, and Kieran MW (2008). Anti-apoptosis mechanisms in malignant gliomas. *J Clin Oncol* **26**, 493–500.
[7] Bromberg J and Darnell Jr JE (2000). The role of STATs in transcriptional control and their impact on cellular function. *Oncogene* **19**, 2468–2473.
[8] Yu H and Jove R (2004). The STATs of cancer—new molecular targets come of age. *Nat Rev Cancer* **4**, 97–105.
[9] Weissenberger J, Loeffler S, Kappeler A, Kopf M, Lukes A, Afanasieva TA, Aguzzi A, and Weis J (2004). IL-6 is required for glioma development in a mouse model. *Oncogene* **23**, 3308–3316.
[10] Gray GK, McFarland BC, Nozell SE, and Benveniste EN (2014). NF-kappaB and STAT3 in glioblastoma: therapeutic targets coming of age. *Expert Rev Neurother* **14**, 1293–1306.
[11] Birner P, Toumangelova-Uzeir K, Natchev S, and Guentchev M (2010). STAT3 tyrosine phosphorylation influences survival in glioblastoma. *J Neurooncol* **100**, 339–343.
[12] Priester M, Copanaki E, Vafaizadeh V, Hensel S, Bernreuther C, Glatzel M, Seifert V, Groner B, Kogel D, and Weissenberger J (2013). STAT3 silencing inhibits glioma single cell infiltration and tumor growth. *Neuro Oncol* **15**, 840–852.
[13] Weissenberger J, Priester M, Bernreuther C, Rakel S, Glatzel M, Seifert V, and Kogel D (2010). Dietary curcumin attenuates glioma growth in a syngeneic mouse model by inhibition of the JAK1,2/STAT3 signaling pathway. *Clin Cancer Res* **16**, 5781–5795.
[14] Chen F, Xu Y, Luo Y, Zheng D, Song Y, Yu K, Li H, Zhang L, Zhong W, and Ji Y (2010). Down-regulation of Stat3 decreases invasion activity and induces apoptosis of human glioma cells. *J Mol Neurosci* **40**, 353–359.
[15] Li GH, Wei H, Chen ZT, Lv SQ, Yin CL, and Wang DL (2009). STAT3 silencing with lentivirus inhibits growth and induces apoptosis and differentiation of U251 cells. *J Neurooncol* **91**, 165–174.
[16] Rahaman SO, Harbor PC, Chernova O, Barnett GH, Vogelbaum MA, and Haque SJ (2002). Inhibition of constitutively active Stat3 suppresses proliferation and induces apoptosis in glioblastoma multiforme cells. *Oncogene* **21**, 8404–8413.
[17] Kroemer G, Galluzzi L, and Brenner C (2007). Mitochondrial membrane permeabilization in cell death. *Physiol Rev* **87**, 99–163.
[18] Adams JM and Cory S (2007). The Bcl-2 apoptotic switch in cancer development and therapy. *Oncogene* **26**, 1324–1337.
[19] Cory S and Adams JM (2002). The Bcl2 family: regulators of the cellular life-or-death switch. *Nat Rev Cancer* **2**, 647–656.
[20] Chao DT and Korsmeyer SJ (1998). BCL-2 family: regulators of cell death. *Annu Rev Immunol* **16**, 395–419.
[21] Lessene G, Czabotar PE, and Colman PM (2008). BCL-2 family antagonists for cancer therapy. *Nat Rev Drug Discov* **7**, 989–1000.
[22] Billard C (2013). BH3 mimetics: status of the field and new developments. *Mol Cancer Ther* **12**, 1691–1700.
[23] Oltersdorf T, Elmore SW, Shoemaker AR, Armstrong RC, Augeri DJ, Belli BA, Bruncko M, Deckwerth TL, Dinges J, and Hajduk PJ, et al (2005). An inhibitor of Bcl-2 family proteins induces regression of solid tumours. *Nature* **435**, 677–681.
[24] Tse C, Shoemaker AR, Adickes J, Anderson MG, Chen J, Jin S, Johnson EF, Marsh KC, Mitten MJ, and Nimmer P, et al (2008). ABT-263: a potent and orally bioavailable Bcl-2 family inhibitor. *Cancer Res* **68**, 3421–3428.
[25] Hetschko H, Voss V, Horn S, Seifert V, Prehn JH, and Kogel D (2008). Pharmacological inhibition of Bcl-2 family members reactivates TRAIL-induced apoptosis in malignant glioma. *J Neurooncol* **86**, 265–272.
[26] Voss V, Senft C, Lang V, Ronellenfitsch MW, Steinbach JP, Seifert V, and Kogel D (2010). The pan-Bcl-2 inhibitor (-)-gossypol triggers autophagic cell death in malignant glioma. *Mol Cancer Res* **8**, 1002–1016.
[27] Sheng Z, Li L, Zhu LJ, Smith TW, Demers A, Ross AH, Moser RP, and Green MR (2010). A genome-wide RNA interference screen reveals an essential CREB3L2-ATF5-MCL1 survival pathway in malignant glioma with therapeutic implications. *Nat Med* **16**, 671–677.
[28] Yoo JY, Wang W, Desiderio S, and Nathans D (2001). Synergistic activity of STAT3 and c-Jun at a specific array of DNA elements in the alpha 2-macroglobulin promoter. *J Biol Chem* **276**, 26421–26429.
[29] Iwamaru A, Szymanski S, Iwado E, Aoki H, Yokoyama T, Fokt I, Hess K, Conrad C, Madden T, and Sawaya R, et al (2007). A novel inhibitor of the STAT3 pathway induces apoptosis in malignant glioma cells both in vitro and in vivo. *Oncogene* **26**, 2435–2444.
[30] Li J, Chen Y, Wan J, Liu X, Yu C, and Li W (2014). ABT-263 enhances sorafenib-induced apoptosis associated with Akt activity and the expression of Bax and p21((CIP1/WAF1)) in human cancer cells. *Br J Pharmacol* **171**, 3182–3195.
[31] Kharaziha P, Rodriguez P, Li Q, Rundqvist H, Bjorklund AC, Augsten M, Ullen A, Egevad L, Wiklund P, and Nilsson S, et al (2012). Targeting of distinct signaling cascades and cancer-associated fibroblasts define the efficacy of Sorafenib against prostate cancer cells. *Cell Death Dis* **3**, e262.
[32] Yang F, Brown C, Buettner R, Hedvat M, Starr R, Scuto A, Schroeder A, Jensen M, and Jove R (2010). Sorafenib induces growth arrest and apoptosis of human glioblastoma cells through the dephosphorylation of signal transducers and activators of transcription 3. *Mol Cancer Ther* **9**, 953–962.
[33] Konopleva M, Contractor R, Tsao T, Samudio I, Ruvolo PP, Kitada S, Deng X, Zhai D, Shi YX, and Sneed T, et al (2006). Mechanisms of apoptosis sensitivity and resistance to the BH3 mimetic ABT-737 in acute myeloid leukemia. *Cancer Cell* **10**, 375–388.
[34] Lucas KM, Mohana-Kumaran N, Lau D, Zhang XD, Hersey P, Huang DC, Weninger W, Haass NK, and Allen JD (2012). Modulation of NOXA and MCL-1 as a strategy for sensitizing melanoma cells to the BH3-mimetic ABT-737. *Clin Cancer Res* **18**, 783–795.
[35] Hikita H, Takehara T, Shimizu S, Kodama T, Shigekawa M, Iwase K, Hosui A, Miyagi T, Tatsumi T, and Ishida H, et al (2010). The Bcl-xL inhibitor, ABT-737, efficiently induces apoptosis and suppresses growth of hepatoma cells in combination with sorafenib. *Hepatology* **52**, 1310–1321.
[36] Siegelin MD, Raskett CM, Gilbert CA, Ross AH, and Altieri DC (2010). Sorafenib exerts anti-glioma activity in vitro and in vivo. *Neurosci Lett* **478**, 165–170.
[37] Blechacz BR, Smoot RL, Bronk SF, Werneburg NW, Sirica AE, and Gores GJ (2009). Sorafenib inhibits signal transducer and activator of transcription-3 signaling in cholangiocarcinoma cells by activating the phosphatase shatterproof 2. *Hepatology* **50**, 1861–1870.